Deep Learning-Based Signal Classification in Wireless Fading Channels

Beza Negash Getu
Department of Electrical & Electronics Engineering (EEE), American University of Ras Al Khaimah, Ras Al Khaimah, UAE
bgetu@aurak.ac.ae (corresponding author)

Ali Al-Ataby
Department of Electrical & Electronics Engineering (EEE), American University of Ras Al Khaimah, Ras Al Khaimah, UAE
ali.ataby@aurak.ac.ae

Hussain Attia
Department of Electrical & Electronics Engineering (EEE), American University of Ras Al Khaimah, Ras Al Khaimah, UAE
hattia@aurak.ac.ae

Received: 7 September 2025 | Revised: 2 October 2025 | Accepted: 12 October 2025

ABSTRACT

Signal detection and identification are critical in today's shared wireless communication environments with diverse devices. These processes are fundamental to wireless, satellite, cognitive radio, and military communication systems. Automatic and real-time identification of radio traffic enables efficient utilization of resources, such as transmission bandwidth and power. It also facilitates dynamic spectrum access by identifying unused spectrum bands and maintaining fair coexistence among the communication devices. Furthermore, it contributes to spectrum surveillance by detecting unknown or unauthorized transmissions, and, hence, enhancing the Quality of Service (QoS) and network performance through effective noise and interference detection and mitigation. In this work, a Deep Learning (DL) approach is proposed for feature extraction and classification of received signals. In particular, a Convolutional Neural Network (CNN) is employed to classify multiple modulation schemes in wireless fading channel conditions. Simulation results show that the CNN provides high classification accuracy, indicating the effectiveness of the proposed method in realistic wireless channels.

Keywords-signal detection; signal identification; Deep Learning (DL); modulation; fading channels; classification; Convolutional Neural Network (CNN)

I. INTRODUCTION

In today's increasingly connected world, wireless systems and services are expanding very rapidly, which makes the ability to detect and identify signals crucial for ensuring efficient, reliable, and secure communication. As wireless networks grow in a more complex and adaptive way, and with increasing demands on spectrum usage, signal detection and identification become more critical than before. These functions allow systems to determine not only the presence of a signal in the communication medium but also its type and characteristics, enabling intelligent decision-making in a wide range of scenarios, from cognitive radio networks to military surveillance and electronic warfare [1, 2]. Signal detection involves determining whether a signal exists in a noisy environment, which is a fundamental step for tasks such as synchronization, channel estimation, and initial access in communication systems [3]. Signal identification goes beyond that by classifying the detected signal according to features such as modulation type, protocol, or source. This process is especially important in environments where multiple technologies and users share the same spectrum [4]. With the advent of cognitive radio and dynamic spectrum access, signal identification enables secondary users to detect and exploit unused frequency bands without interfering with licensed (primary) users [5].

Beyond efficiency, signal identification plays an important role in security. It enables the detection of unauthorized or potentially malicious transmissions in cognitive radio networks [6], supports threat assessment and countermeasure strategies in military operations [7], and enhances the Quality of Service (QoS) in civilian networks by improving spectrum management and ensuring regulatory compliance. The utilization of Machine Learning (ML) and, subsequently, Deep Learning (DL) has improved the speed and accuracy of signal detection and classification remarkably, even under challenging conditions such as low Signal-to-Noise Ratios (SNRs) [8].

As wireless technology evolves toward the fifth generation (5G) and sixth generation (6G), these capabilities become even more vital, necessitating the development of intelligent, adaptive, and resilient communication systems. The widespread deployment of 5G wireless networks has significantly enhanced QoS and user experience across a wide range of applications. Looking forward, 6G networks are expected to become widespread within the next decade, overcoming the limitations of 5G and opening the door to a new era of communication [9, 10]. Future wireless systems will be required to deliver higher capacity, faster data rates, lower latency, enhanced security, and more robust QoS than current 5G networks. Driven by advances in Artificial Intelligence (AI), 6G is anticipated to transform global wireless communication by enabling ultra-low-latency connectivity, massive device integration, and unprecedented internet speeds. These features will be implemented through terrestrial, aerial, and maritime communication platforms that form a unified intelligent network infrastructure [11]. To achieve these goals, 6G will rely on a combination of key technologies, use cases, ML tools, communication protocols, networking architectures, and computing paradigms [12]. As the diversity of wireless technologies and the number of connected users grow, the demand for advanced and intelligent solutions capable of maintaining system efficiency, scalability, and adaptability will also increase. In this context, ML and DL will play a crucial role. These techniques offer powerful tools for optimizing dynamic, time-varying network environments and are essential for supporting the increasingly complex applications required for 5G and 6G. Among the many critical capabilities, signal detection and identification will remain necessary for ensuring the efficient operation of shared wireless systems [13].

A DL-based Automatic Modulation Classification (AMC) framework for 6G communication was proposed by authors in [14]. This approach used pre-trained CNN models (ResNet18 and ResNet101) to classify eight types of digital modulation. It employed LabVIEW NXG to simulate transceivers operating at 100 GHz, a typical carrier frequency of 6G. The opportunities and challenges of DL in 6G have been comprehensively discussed by authors in [15], highlighting approaches for integrating DL into 6G networks. The study reviewed how DL models, such as Convolutional Neural Networks (CNNs), Generative Adversarial Networks (GANs), Graph Neural Networks (GNNs), Deep Reinforcement Learning (DRL), Transformers, Federated Learning (FL), and meta-learning, along with AI-Generated Content (AIGC), can play a role in 6G systems. In addition, a comprehensive survey of AI technologies applied across various wireless networks and applications was presented by authors in [16].

Authors in [17] presented a strategic vision for 6G using Frequency Range 3 (FR3). The study explored spectrum agility strategies and coexistence among systems such as satellite communications and radio astronomy. In addition, authors in [17] discussed the role of massive Multiple-Input Multiple-Output (MIMO) technologies, deployment challenges, and solutions such as multiband sensing for integrated communication systems. A novel CNN-based method was proposed by authors in [18] to estimate the velocity and range of moving targets through range–Doppler maps. The study evaluated the effectiveness of the proposed method by comparing it with traditional techniques such as the 2D periodogram, 2DResFreq, and VGG-19. The proposed method demonstrated higher estimation accuracy for different SNR levels, faster prediction times, and enhanced image quality.

Recent years have seen an increased research emphasis on the application of ML and DL techniques to the problems of signal detection and identification. For example, authors in [19] investigated the use of DL for multi-signal detection and modulation classification, which are fundamental requirements for many modern communication systems. These techniques enable communication systems to automatically classify modulation formats, configure parameters, and adapt to dynamic and shared communication environments. DL methods offer unique advantages over traditional energy-based wideband signal detection techniques, which often rely on thresholds and tend to perform poorly in noisy or low SNR conditions. Due to their self-learning capabilities, DL models can extract and learn complex features directly from raw input data, making them more robust and efficient in challenging environments.

Accurate signal type identification is particularly important in shared-spectrum networks, where intelligent resource allocation and fair coexistence among users are essential. For example, signal classification can be used to schedule signal transmissions, prevent signal collisions, and improve overall system efficiency [20]. Among various DL architectures, CNNs have emerged as a powerful tool for many classification problems. CNNs were originally developed for image analysis and are capable of learning spatial patterns of features through layers of convolution, pooling, and non-linear activation functions. Furthermore, traditional approaches depend on selected features, whereas CNNs automatically extract high-level representations from raw data, resulting in high classification accuracy across a wide range of tasks [21]. The architectural characteristics of CNNs, such as local receptive fields and weight sharing, enable them to efficiently learn spatially invariant patterns, making them highly effective in applications such as object recognition, medical image analysis, autonomous systems, and remote sensing [22, 23]. The success of CNNs in these domains indicates their potential in signal classification, especially when dealing with complex and noisy communication environments.

Authors in [24] focused on Electroencephalogram (EEG) signal identification using a single-layer neural network. The EEG signals were first transformed into images using wavelet decomposition, and the model achieved a high classification accuracy of over 90%. Authors in [25] used DL-based wireless signal classification in an Internet of Things (IoT) environment containing Wi-Fi, Bluetooth, and ZigBee devices, using CNN and Long Short-Term Memory (LSTM) networks to learn spatial and temporal signal features. LSTM networks are capable of capturing both short-term and long-term time dependencies, making them well-suited for modeling and predicting nonlinear, time-variant system dynamics, such as signal variations in the presence of additive noise [26]. Authors in [27] proposed the use of a CNN trained on spectrograms of Binary Phase Shift Keying (BPSK) and Quadrature Phase Shift Keying (QPSK) modulation schemes. The study concluded that the proposed CNN-based framework effectively classifies modulation schemes in Vehicle-to-Everything (V2X) communications.

In this work, we investigate the use of CNNs for the identification and classification of signals modulated using M-ary Phase Shift Keying (MPSK), M-ary Amplitude Phase Shift Keying (MAPSK), and M-ary Quadrature Amplitude Modulation (MQAM) under transmission channel impairments such as fading and Additive White Gaussian Noise (AWGN). Wireless communication channels are inherently unpredictable due to fading, which results from the multipath propagation of radio signals. Fading can be categorized into two types: large-scale fading, caused by path loss and shadowing over long distances, and small-scale fading, resulting from rapid fluctuations in signal amplitude and phase over short distances or short intervals [28]. Modeling these effects accurately is essential when implementing robust wireless systems, especially in high-mobility environments such as vehicular or satellite communication systems. Many fading models, such as Rayleigh, Rician, and Nakagami, have been developed to characterize different propagation scenarios [29-31]. These models play a crucial role in the evaluation and optimization of communication systems, influencing modulation, coding, diversity, and antenna design. Hence, considering realistic fading characteristics is important for assessing the performance and reliability of wireless fading radio channels.

The main contributions of this study are summarized as follows:

- Applying DL techniques to extract features from the received signals and perform automatic signal classification.
- Evaluating the effectiveness of CNNs in the classification of various modulation schemes.
- Enhancing the functionality of modern wireless communication systems by improving signal detection and identification and supporting efficient and intelligent spectrum utilization. In view of this, modern wireless systems can benefit from CNN-based classification techniques by enabling the autonomous management of complex networks through real-time data analysis, pattern recognition, and resource optimization.

II. METHODS

The system under consideration is illustrated in Figure 1. It consists of two main parts: signal generation and channel impairment modeling. An input data source in the form of bits or symbols is digitally modulated first and mapped to the appropriate modulation scheme, such as BPSK, QPSK, 16-QAM, and then the symbol sequence (a_n) passes through an appropriate square-root raised cosine filter ($g(t)$). The filtered signal passes through a mixer or carrier modulator that has a local oscillator with a carrier frequency f_c and phase ϕ. The resulting signal then passes through the wireless fading channel, and the channel adds AWGN to the received signal and produces the output, $y(t)$.

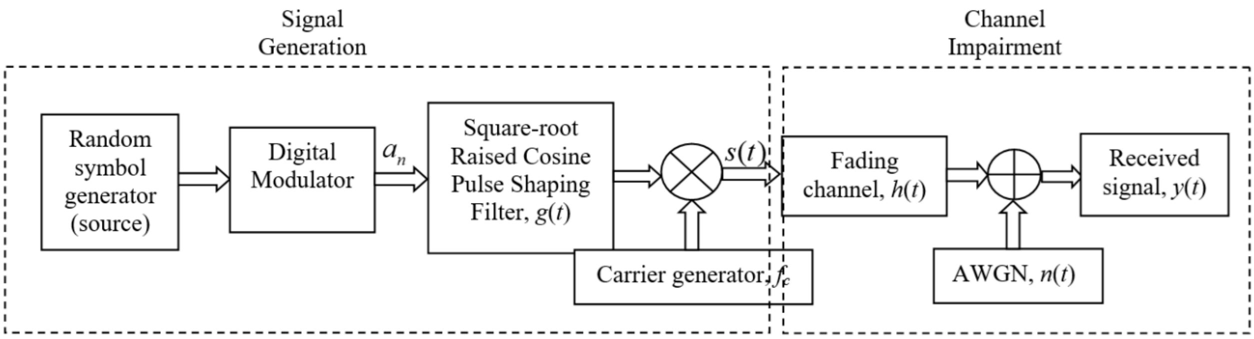

Fig. 1. Block diagram of the signal generation and channel impairment modeling.

The complex-valued transmitted signal $s(t)$ after the carrier modulation can be represented as:

$$s(t)=\sum_{n=-\infty}^{\infty} a_n g(t-nT)e^{j(2\pi f_c t+\phi)} \quad (1)$$

where T is the symbol time, a_n is the digitally modulated symbol sequence during the n-th symbol period, and $g(t)$ is the square-root raised cosine shaping filter. For MPSK, the symbol sequence is given as:

$$a_n = e^{j(\frac{2\pi n}{M}+\phi_0)},\ \ n\in\{0, 1, 2, \cdots, M-1\} \quad (2)$$

where M specifies the modulation order and ϕ_0 specifies the phase offset of the MPSK constellation. The mapping of digital message to MPSK symbols can be done either from integers to MPSK symbols or from bit sequences to MPSK symbols. In the latter case, the bit sequences are first converted to integers either by using Gray code, standard binary code, or any other binary code transformation scheme, where the number of bits per symbol is $m=\log_2 M$. For MQAM digital modulated signals, the symbol sequence is:

$$a_n = a_{nI} + ja_{nQ} \quad (3)$$

where a_{nI} and a_{nQ} are the in-phase and quadrature phase components, respectively. For rectangular QAM, the symbol sequence is:

$$a_{nI}, a_{nQ} = 2i - \tfrac{M}{4} + 1, \quad i = 0, 1, \ldots, \tfrac{M}{4} - 1 \qquad (4)$$

where $M = 2^m$. For M-ary Pulse Amplitude Modulation (MPAM) modulation, the symbol sequence is:

$$a_n = 2i - 1 - M, \quad i = 1, 2, \ldots, M \qquad (5)$$

Similar mathematical equations for other modulation schemes are available in the literature.

The dataset used in this study was generated based on the process shown in Figure 1. Rician and Rayleigh fading channel impairments were applied to the data to simulate realistic transmission conditions. The classification tasks were performed using a CNN implemented in MATLAB. The CNN consists of five convolution layers and one fully connected layer. Each convolutional layer except the last is followed by a batch normalization layer, Rectified Linear Unit (ReLU) activation layer, and max pooling layer. In the last convolutional layer, the max pooling layer is replaced with a global average pooling layer. The pooling layer reduces the number of learnable parameters and the amount of computation performed in the network. The output layer has a softmax activation function for the modulation classification tasks. The structure of the CNN used in this study is provided in Table I.

III. SIMULATIONS

The simulation dataset was generated to include a diverse set of modulation types, namely BPSK, QPSK, 8-PSK, 16-QAM, 64-QAM, PAM-4, Gaussian Frequency Shift Keying (GFSK), and Continuous-Phase Frequency Shift Keying (CPFSK). For training purposes, 10,000 frames were generated for each modulation type, with each frame consisting of 1024 samples. The digitally modulated signals were passed through a square-root raised cosine pulse shaping filter with a roll-off factor $\beta = 0.35$, followed by the mixer and the fading channel, as described in Figure 1. To model realistic channel impairments, the fading channel was generated using the comm.RicianChannel system object in MATLAB. The K-factor of the fading channel varied from a negligibly small value (Rayleigh fading) to strong Line of Sight (LoS) scenarios for the Rician fading. The fading was assumed to vary from frame to frame to simulate dynamic channel conditions. A center frequency of transmission $f_c = 900$ MHz and a sampling rate of $f_s = 200$ kHz were considered. In addition to channel fading and additive noise, the simulation also accounted for oscillator inaccuracies. A clock offset of up to 5 parts per million (ppm) was assumed. For each frame, the channel generated a random clock offset value obtained from a uniformly distributed set of values over the full offset range. As a reference case, the ideal condition with zero clock offset and no carrier frequency or sampling time drift was also simulated.

For the Rician fading channel, a three-path propagation model was adopted with path gains [0, −3, −12 dB] and corresponding path delays [0, 1.2, 3.5] / f_s. A maximum Doppler shift of 4.5 Hz was applied to the LoS component, representing an average pedestrian mobility speed of 1.5 m/s. The Rayleigh fading channel was simulated using MATLAB's comm.RicianChannel object with a K-factor value of -200 dB (or 10^{-20} in linear scale, approximately zero), effectively eliminating any dominant LoS component. The average SNR was 30 dB. Before training, the frames for each modulation type were generated, stored, and split into 80% for the training, 10% for validation, and 10% for testing the CNN.

TABLE I. CNN ARCHITECTURE FOR MODULATION CLASSIFICATION

Layer	Type	Parameters
Input	1D Signal	1024 samples per frame, normalization="zscore"
Conv1	Conv1D	filterSize=8, numFilters=16, stride=1, padding='same'
BatchNorm1	Batch normalization	
ReLU1	Rectified linear unit activation layer	
MaxPooling1	MaxPooling1D	poolSize=2, stride=2, padding=[0 0]
Conv2	Conv1D	filterSize=8, numFilters=32, stride=1, padding='same'
BatchNorm2	Batch normalization	
ReLU2	Rectified linear unit activation layer	
MaxPooling2	MaxPooling1D	poolSize=2, stride=2, padding=[0 0]
Conv3	Conv1D	filterSize=8, numFilters=48, stride=1, padding='same'
BatchNorm3	Batch normalization	
ReLU3	Rectified linear unit activation layer	
MaxPooling3	MaxPooling1D	poolSize=2, stride=2, padding=[0 0]
Conv4	Conv1D	filterSize=8, numFilters=64, stride=1, padding= 'same'
BatchNorm4	Batch normalization	
ReLU4	Rectified linear unit activation layer	
MaxPooling4	MaxPooling1D	poolSize=2, stride=2, padding=[0 0]
Conv5	Conv1D	filterSize=8, numFilters=32, stride=1, padding='same'
BatchNorm5	Batch normalization	
ReLU5	Rectified linear unit activation layer	
GlobalAvgPooling	Pooling	
Fully connected	Dense	Units=8 (for 8 modulation classes)
Output	Softmax	

IV. RESULTS AND DISCUSSION

Figure 2 shows the training results for SNR = 30 dB and a channel with K = 5 (linear scale). Each modulation type included 10,000 frames split into 80% for training, 10% for validation, and 10% for testing. Data generation and training took over 3.5 h, with the training phase lasting 2 h 20 min. Both training and validation accuracies exceeded 90%, confirming effective learning and generalization. The trained CNN classifier was then used to classify the 1,000 test frames per modulation type.

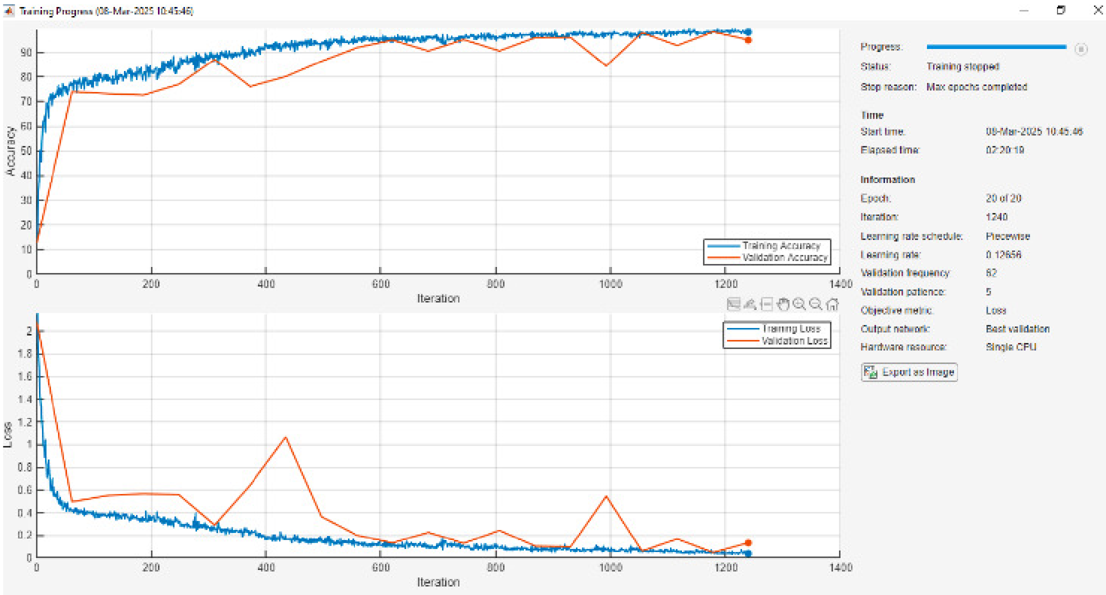

Fig. 2. Training results for the dataset (10,000 frames per modulation type).

Figure 3 shows the resulting confusion matrix, demonstrating testing accuracy above 98% for all modulation types, except for 64-QAM, which achieved 92.7%. The small confusion value between 64-QAM and 16-QAM is due to the similarity of their signal constellation diagrams. Obviously, a larger dataset would reduce this inaccuracy. Overall, the average test accuracy over all modulation types was 98.3%, which is a significant achievement.

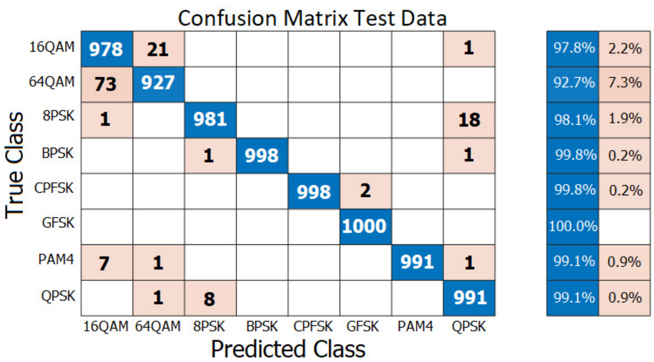

Fig. 3. Confusion matrix for test signals (1,000 frames per modulation type) under multi-path Rician fading ($K = 5$).

The trained CNN model, developed using 10,000 frames per modulation type, was saved in a MATLAB file and later used to classify different sets of randomly generated input frames following the procedure outlined in Section III.

Figure 4 shows the classification results when the trained network was provided with 200 frames per modulation type. The average test accuracy in this case was 98.125%, with several modulation types achieving 100% accuracy. This shows the robustness and generalization capability of the trained network in classifying unseen data.

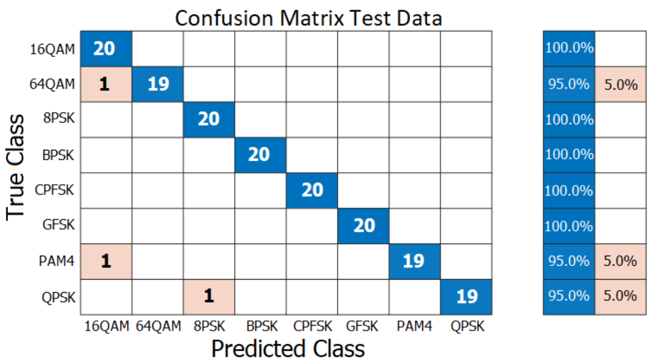

Fig. 4. Confusion matrix for test signals (200 frames per modulation type) under multi-path Rician fading ($K = 5$).

In the next experiment, a Rician fading channel with a single path, average path gain of 0 dB, path delay of 0 s, and K-factor of 5 was considered. The clock offset and resulting frequency and sampling time shift were kept the same as before. A new dataset was generated under these conditions, and the saved trained network was used for classification. The average test accuracy for this case was also found to be 98.125%, with seven out of eight modulation types achieving 100% accuracy, as shown in Figure 5. This high performance is expected given the simplicity of the one-path Rician fading channel model.

The fourth experiment was conducted using a single-path Rayleigh fading channel. The K-factor was set to −200 dB, which is 10^{-20} in linear scale (nearly equal to zero), effectively simulating a Rayleigh scenario. Figure 6 shows the classification results for 200 input frames per modulation type. The average test accuracy for this case was 96.25%, lower than the Rician fading scenario, as expected due to the severity of the impairments in Rayleigh fading compared to the Rician fading. There is some confusion between BPSK and QPSK, as expected, due to the similarity of their constellations, especially under fading conditions that distort phase information.

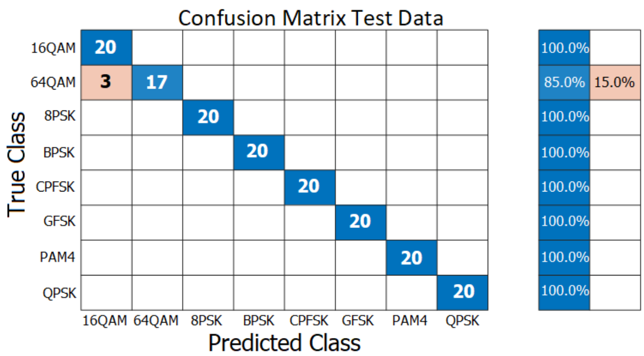

Fig. 5. Confusion matrix for the one-path Rician fading model.

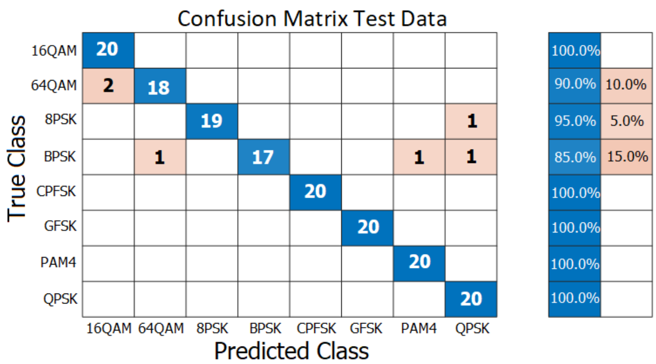

Fig. 6. Confusion matrix for the one-path Rayleigh fading model.

The final experiment was conducted under ideal conditions, with no clock offset, no carrier frequency shift, and perfect sampling time, to serve as a baseline reference for performance evaluation. The channel was a Rician fading channel with three paths, path gains of [0, −3 dB, −12 dB], and corresponding path delays of [0, 1.2, 3.5] / f_s. The trained network was used to classify the test frames generated under these conditions.

Training was performed with 10,000 frames per modulation type, with 80% used for training, 10% for validation, and 10% for testing. Figure 7 shows the classification results, with a test accuracy of 98.8125%, indicating a negligible improvement compared to the results with the clock offset. This shows the robustness of the CNN and its generalization capability in capturing different features of the dataset.

Table II presents the classification performance under different channel conditions. Overall accuracy was high (>96%) for all scenarios, indicating that the proposed model is robust under different fading environments. Classification accuracy for 64-QAM was consistently lower than other modulation schemes, with the most confusion occurring between 64-QAM and 16-QAM due to the similarity of their constellation structures. This pattern was especially evident in the one-path Rician fading scenario, where 64-QAM accuracy dropped to 85%, indicating that the lack of diversity in multipath propagation makes it harder to distinguish closely spaced constellations. In the Rayleigh fading case, although 64-QAM performs better than in the one-path Rician scenario, confusion arose between BPSK and QPSK, which share phase-based features that can overlap under severe fading. The ideal scenario (no clock offsets) yielded the highest overall accuracy of 98.8%, confirming that synchronization impairments slightly affect classification performance.

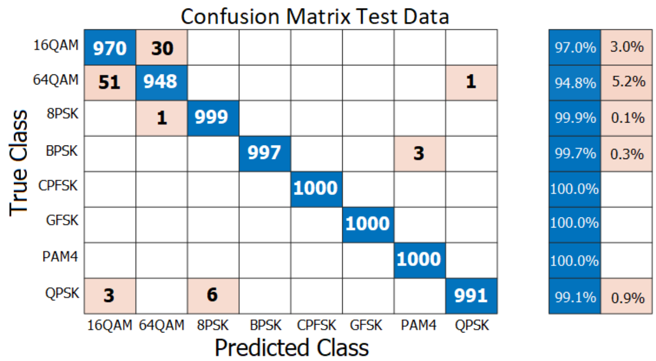

Fig. 7. Confusion matrix for test frames under ideal conditions with no clock offset.

TABLE II. CLASSIFICATION PERFORMANCE UNDER DIFFERENT CHANNEL CONDITIONS

Scenario	Accuracy (%)	64-QAM accuracy (%)	Most confused modulation pair
Three-path Rician (K=5)	98.1	95.0	64-QAM vs 16-QAM
One-path Rician (K=5)	98.1	85.0	64-QAM vs 16-QAM
Rayleigh ($K \approx 0$)	96.3	90.0	BPSK vs QPSK
Ideal (no clock offset)	98.8	94.8	64-QAM vs 16-QAM

These observations highlight both the strength of the CNN model and the inherent challenges in distinguishing higher-order modulations under limited or distorted channel conditions. The results demonstrate that DL models, such as CNNs, can automatically extract relevant and complex features from raw signal data and perform accurate classifications. They achieve superior recognition accuracy even under challenging conditions, such as noisy and wireless fading channels. Their ability to learn intricate patterns makes DL-based systems more resilient to signal variability and noise, improving performance compared to traditional approaches. Deep neural networks can be scaled to process large datasets and are adaptable to various communication scenarios, making them a powerful tool for large-scale applications. Although the results show high accuracy in MATLAB simulations, such highly accurate performance is not expected in practice, as the radio channel model could differ, channels may be highly time-variant, and performance may be limited by interference from other users.

A CNN-based AMC pipeline similar to the proposed in this work can be deployed Over-the-Air (OTA) using Software-Defined Radios (SDRs), as prior studies have shown strong real-world performance for DL classifiers trained on I/Q samples. To generalize the results of this study beyond simulation, standardized channel models (e.g., 3GPP TR 38.901) can be adopted during data generation. Also, training can be augmented with RF impairments (CFO, phase noise, IQ imbalance), or compensated via a lightweight DSP front-end. Finally, fine-tuning on small OTA corpora, such as RadioML-style captures, can be performed before field deployment. For on-device spectrum sensing and dynamic spectrum access, 1D-CNNs with short input windows (e.g., 1,024 samples) meet tight latency requirements on embedded SDR platforms after quantization. Incorporating these steps (TR 38.901 profiles, impairment augmentation, and OTA fine-tuning) is planned for future work to quantify domain transfer, end-to-end latency, and accuracy.

V. CONCLUSIONS

Signal detection and identification play a pivotal role in enhancing the reliability, efficiency, and adaptability of modern wireless communication systems. By accurately recognizing the presence and type of signals in complex and often dynamic environments, these techniques enable critical functions such as interference management, spectrum sensing, and adaptive resource allocation. The integration of advanced algorithms, particularly those based on Machine Learning (ML) and Deep Learning (DL), has significantly improved detection accuracy and robustness, especially under low Signal-to-Noise Ratio (SNR) conditions and non-stationary channels. As wireless technologies evolve toward sixth generation (6G) and beyond, the demand for intelligent, real-time signal identification methods will continue to grow, supporting applications in cognitive radio, autonomous systems, and secure communications. Ongoing research in this area is essential to meet the increasing performance requirements and complexity of next-generation wireless networks.

In this work, we have demonstrated the identification and classification of various modulation types using a Convolutional Neural Network (CNN). Synthetic datasets were generated by introducing fading channel impairments, Additive White Gaussian Noise (AWGN), and frequency and sampling time shifts. The generated datasets were used to train the CNN for classification. MATLAB simulation results showed test accuracy exceeding 98% in classification. Different channel fading scenarios were evaluated, and the CNN successfully identified and classified the modulation types, consistently achieving a test accuracy above 98%. The ideal scenario with no clock offset was also investigated, and similar results were obtained. The results demonstrate the robustness of the CNN in capturing different features of the modulation dataset and achieving high classification accuracy.

Automatic identification of Over-the-Air (OTA) signals is essential in wireless communication, as the medium is becoming increasingly shared and crowded, with a rapidly growing number of wireless devices competing for available radio spectrum and resources. From this perspective, it is evident that wireless networks equipped with Artificial Intelligence (AI) and DL networks will play a crucial role in the management of devices and resources in future wireless networks.

DISCLOSURE STATEMENT

No potential conflict of interest was reported by the authors.

DATA AVAILABILITY STATEMENT

The data generation process and the dataset used for the simulations are described in this paper; however, the authors agree to make the dataset available upon request.

REFERENCES

[1] S. Haykin, "Cognitive radio: brain-empowered wireless communications," *IEEE Journal on Selected Areas in Communications*, vol. 23, no. 2, pp. 201–220, Feb. 2005, https://doi.org/10.1109/JSAC.2004.839380.

[2] A. Swami and B. M. Sadler, "Hierarchical digital modulation classification using cumulants," *IEEE Transactions on Communications*, vol. 48, no. 3, pp. 416–429, Mar. 2000, https://doi.org/10.1109/26.837045.

[3] H. V. Poor, *An Introduction to Signal Detection and Estimation*. New York, NY, USA: Springer, 1994, https://doi.org/10.1007/978-1-4757-2341-0.

[4] M. Oner and F. Jondral, "Air interface recognition for a software radio system exploiting cyclostationarity," in *2004 IEEE 15th International Symposium on Personal, Indoor and Mobile Radio Communications*, Barcelona, Spain, 2004, pp. 1947-1951 vol.3, https://doi.org/10.1109/PIMRC.2004.1368338.

[5] I. F. Akyildiz, W.-Y. Lee, M. C. Vuran, and S. Mohanty, "NeXt generation/dynamic spectrum access/cognitive radio wireless networks: A survey," *Computer Networks*, vol. 50, no. 13, pp. 2127–2159, Sept. 2006, https://doi.org/10.1016/j.comnet.2006.05.001.

[6] A. G. Fragkiadakis, E. Z. Tragos, and I. G. Askoxylakis, "A Survey on Security Threats and Detection Techniques in Cognitive Radio Networks," *IEEE Communications Surveys & Tutorials*, vol. 15, no. 1, pp. 428–445, 2013, https://doi.org/10.1109/SURV.2011.122211.00162.

[7] A. E. Spezio, "Electronic warfare systems," *IEEE Transactions on Microwave Theory and Techniques*, vol. 50, no. 3, pp. 633–644, Mar. 2002, https://doi.org/10.1109/22.989948.

[8] P. He, Y. Zhang, X. Yang, X. Xiao, H. Wang, and R. Zhang, "Deep Learning-Based Modulation Recognition for Low Signal-to-Noise Ratio Environments," *Electronics*, vol. 11, no. 23, Dec. 2022, Art. no. 4026, https://doi.org/10.3390/electronics11234026.

[9] E. A. Kadir, R. Shubair, S. K. Abdul Rahim, M. Himdi, M. R. Kamarudin, and S. L. Rosa, "B5G and 6G: Next Generation Wireless Communications Technologies, Demand and Challenges," in *2021 International Congress of Advanced Technology and Engineering*, Taiz, Yemen, 2021, pp. 1–6, https://doi.org/10.1109/ICOTEN52080.2021.9493470.

[10] M. Z. Asghar, S. A. Memon, and J. Hämäläinen, "Evolution of Wireless Communication to 6G: Potential Applications and Research Directions," *Sustainability*, vol. 14, no. 10, May 2022, Art. no. 6356, https://doi.org/10.3390/su14106356.

[11] N. Telagam, N. Kandasamy, A. K. Manoharan, P. Anandhi, and R. Atchudan, "Beyond 5G: Exploring key enabling technologies, use cases, and future prospects of 6 G communication," *Nano Communication Networks*, vol. 43, Mar. 2025, Art. no. 100560, https://doi.org/10.1016/j.nancom.2024.100560.

[12] L. U. Khan, I. Yaqoob, M. Imran, Z. Han, and C. S. Hong, "6G Wireless Systems: A Vision, Architectural Elements, and Future Directions," *IEEE Access*, vol. 8, pp. 147029–147044, 2020, https://doi.org/10.1109/ACCESS.2020.3015289.

[13] S. Sikkanan, S. T., K. P. S., K. M., and S. Mehta, "5G and 6G Wireless Communication," in *Innovative Smart Materials Used in Wireless Communication Technology*, R. Krishan and M. Kaur, Eds. Hershey, PA, USA: IGI Global Scientific Publishing, 2023, https://doi.org/10.4018/978-1-6684-7000-8.ch015.

[14] Z. Z. Yahya, D. M. Ali, and M. Y. Abdallah, "6G Automatic Modulation Classification using Deep Learning Models in the Presence of Channel

Noise, CFO, and PN," *Majlesi Journal of Electrical Engineering*, vol. 18, no. 4, pp. 1–9, Dec. 2024, https://doi.org/10.57647/j.mjee.2024.1804.59.

[15] L. Jiao *et al.*, "Advanced Deep Learning Models for 6G: Overview, Opportunities, and Challenges," *IEEE Access*, vol. 12, pp. 133245–133314, 2024, https://doi.org/10.1109/ACCESS.2024.3418900.

[16] A. Alhammadi *et al.*, "Artificial Intelligence in 6G Wireless Networks: Opportunities, Applications, and Challenges," *International Journal of Intelligent Systems*, vol. 2024, no. 1, Mar. 2024, Art. no. 8845070, https://doi.org/10.1155/2024/8845070.

[17] A. Bazzi, R. Bomfin, M. Mezzavilla, S. Rangan, T. Rappaport, and M. Chafii, "Upper Mid-Band Spectrum for 6G: Vision, Opportunity and Challenges." arXiv, Sept. 08, 2025, https://doi.org/10.48550/arXiv.2502.17914.

[18] M. Delamou, A. Bazzi, M. Chafii, and E. M. Amhoud, "Deep Learning-based Estimation for Multitarget Radar Detection," in *2023 IEEE 97th Vehicular Technology Conference*, Florence, Italy, 2023, pp. 1–5, https://doi.org/10.1109/VTC2023-Spring57618.2023.10200157.

[19] X. Zha, H. Peng, X. Qin, G. Li, and S. Yang, "A Deep Learning Framework for Signal Detection and Modulation Classification," *Sensors*, vol. 19, no. 18, Sept. 2019, Art. no. 4042, https://doi.org/10.3390/s19184042.

[20] W. Zhang, M. Feng, M. Krunz, and A. Hossein Yazdani Abyaneh, "Signal Detection and Classification in Shared Spectrum: A Deep Learning Approach," in *IEEE INFOCOM 2021 - IEEE Conference on Computer Communications*, Vancouver, Canada, 2021, pp. 1–10, https://doi.org/10.1109/INFOCOM42981.2021.9488834.

[21] Y. LeCun, Y. Bengio, and G. Hinton, "Deep learning," *Nature*, vol. 521, no. 7553, pp. 436–444, May 2015, https://doi.org/10.1038/nature14539.

[22] A. Krizhevsky, I. Sutskever, and G. E. Hinton, "ImageNet classification with deep convolutional neural networks," *Communications of the ACM*, vol. 60, no. 6, pp. 84–90, May 2017, https://doi.org/10.1145/3065386.

[23] G. Litjens *et al.*, "A survey on deep learning in medical image analysis," *Medical Image Analysis*, vol. 42, pp. 60–88, Dec. 2017, https://doi.org/10.1016/j.media.2017.07.005.

[24] Q. C. Lam, L. A. T. Nguyen, and H. K. Nguyen, "EEG Signal Identification Using Single-Layer Neural Network," *International Journal on Cybernetics & Informatics*, vol. 5, no. 5, pp. 1–10, Oct. 2016, https://doi.org/10.5121/ijci.2016.5501.

[25] H. Roh, S. Oh, H. Song, J. Han, and S. Lim, "Deep Learning-based Wireless Signal Classification in the IoT Environment," *Computers, Materials & Continua*, vol. 71, no. 3, pp. 5717–5732, Jan. 2022, https://doi.org/10.32604/cmc.2022.024135.

[26] B. N. Getu, "LSTM Based Time Series Forecasting of Noisy Signals," in *16th Asian Conference on Intelligent Information and Database Systems, Proceedings, Part II*, Ras Al Khaimah, UAE, 2024, pp. 133–146, https://doi.org/10.1007/978-981-97-5934-7_12.

[27] H. Ouamna, A. Kharbouche, Z. Madini, and Y. Zouine, "Deep Learning-assisted Automatic Modulation Classification using Spectrograms," *Engineering, Technology & Applied Science Research*, vol. 15, no. 1, pp. 19925–19932, Feb. 2025, https://doi.org/10.48084/etasr.9334.

[28] T. S. Rappaport, *Wireless communications: Principles and Practice*, 2nd ed. Upper Saddle River, NJ, USA: Prentice Hall, 2001.

[29] A. Goldsmith, *Wireless Communications*. Cambridge, UK: Cambridge University Press, 2005, https://doi.org/10.1017/CBO9780511841224.

[30] M. K. Simon and M.-S. Alouini, *Digital Communication over Fading Channels*, 2nd ed. Hoboken, NJ, USA: John Wiley & Sons, 2005, https://doi.org/10.1002/0471715220.

[31] B. N. Getu and J. B. Andersen, "MIMO Systems in Random Uncorrelated, Correlated and Deterministic Radio Channels," *Wireless Personal Communications*, vol. 30, no. 1, pp. 27–61, July 2004, https://doi.org/10.1007/s11277-004-4847-x.